

Non-Steady State Gas Permeation Measurements of TiO₂-Doped YSZ

Kiyoshi Kobayashi,* Shu Yamaguchi and Yoshiaki Iguchi

Department of Materials Science and Engineering, Nagoya Institute of Technology Gokiso-cho, Showa-ku, Nagoya 466-8555, Japan

*Present address: Department of Inorganic Materials, National Institute of Materials and Chemical Research Higashi 1-1, Tsukuba, Ibaraki 305-8565, Japan

(Received September 23, 1998)

Mobilities of electrons (μ_n) and holes (μ_p) in 2, 5, and 10 mol% TiO₂-doped yttria stabilized zirconia (TD-YSZ) have been estimated by a non-steady state gas permeation method using models proposed by Weppner and Maruyama. Values of μ_n and μ_p were found to be closed to those in non-doped YSZ reported earlier. The concentration of electrons and holes were calculated from μ_n and μ_p values and the partial conductivities of electrons and holes measured by a dc-polarization method. The concentration of electrons at unit oxygen partial pressure increased with increasing TiO₂ concentration, while the hole concentration was almost independent of TiO₂ concentration.

Key words: Non-steady state gas permeation, Mobility, TiO₂-doped YSZ, Mixed conductor

I. Introduction

Mixed conductors of oxide ion-electron have attracted attentions for the energy conversion materials such as an electrode material for the solid oxide fuel cell (SOFC) and gas permeation membrane.¹⁾ Although the partial conductivity of electrons, σ_n at the same temperature and oxygen partial pressure condition in yttria stabilized zirconia (YSZ) doped with TiO₂ has been known to increase with increasing TiO₂ concentration,¹⁻⁶⁾ it is not clear whether the increase in the concentration of electrons or in the mobility of electrons is responsible for the enhancement of the electronic conductivity. In this study, mobilities of electrons and holes in TiO₂ doped YSZ were estimated from the non-steady state gas permeation measurements and the concentrations of electrons and holes were calculated from the mobilities and the partial conductivities of electronic defects reported earlier.³⁻⁵⁾

II. Experimental

2.1 Experimental procedure

The oxygen gas permeation under non-steady state condition was subjected for 2, 5, and 10 mol% TiO₂ doped YSZ using the Hebb-Wagner's dc-polarization cell with an asymmetric electrode configuration. Details of the cell configurations have been reported earlier.³⁻⁵⁾ Nominal compositions of the samples measured were 90.0 mol% ZrO₂-7.8 mol% Y₂O₃-2.2 mol% TiO₂, 92 mol% ZrO₂-8 mol% Y₂O₃-5 mol% TiO₂, and 87 mol% ZrO₂-8 mol% Y₂O₃-10 mol% TiO₂, and the samples were denoted as 2TD-YSZ, 5TD-YSZ, and 10TD-YSZ, respectively.

The non-steady state oxygen permeation experiment has been made by a current interruption method, where oxygen gas permeates by opening the dc-polarization circuit after a steady state was attained, and the relaxation of the open circuit voltage between reversible electrode and blocking electrode, E_{open} was measured. The experimental runs were made at 1273, 1173, and 1073 K under the unit oxygen fugacity at reversible electrode, $P_{\text{O}_2}^{\text{rev}}$ between $E_{\text{app}}=0.25$ and 1.1 V. Oxygen fugacity at the vicinity of reversible electrode is defined as $P_{\text{O}_2}^{\text{rev}}=(p_{\text{O}_2}^{\text{rev}}/\text{Pa})/(P^\circ/\text{Pa})$, where $p_{\text{O}_2}^{\text{rev}}$ and P° are oxygen partial pressure at the reversible electrode and the standard pressure, 1.01325×10^5 Pa, respectively. E_{open} was measured at intervals of 15 or 30 ms for 5TD-YSZ and 10TD-YSZ, and 5 or 10 s for 2TD-YSZ.

2.2 Mathematical models for the analysis

When the asymmetric cell with blocking and reversible electrodes, which is kept under a steady state at an applied voltage E_{app} is de-polarized by opening the circuit, the slow relaxation of the open circuit voltage, E_{open} is observed due to the electrochemical permeation of oxygen into the small cavity of blocking electrode through the electrolyte. (YSZ in the present case) This oxygen permeation is governed by the internal diffusion of electronic species in the electrolyte. If the transference number of oxide ions ($t_{\text{O}^{2-}}$) is close to unity, theoretical relationships between E_{open} and t can be derived from the Fick's second law,^{7,8)}

$$E_{\text{open}} = E_{\text{app}} - \frac{2RT}{FL} \sqrt{\frac{D_e t}{\pi}}, \quad (\text{when } t \ll \frac{L^2}{D_e}) \quad (1-1)$$

or,

$$E_{\text{open}} = E_{\text{app}} + \frac{RT}{F} \ln \frac{8}{\pi^2} - \frac{D_e \pi^2 RT}{4L^2 F} t, \quad (\text{when } t \gg \frac{L^2}{D_e}) \quad (1-2)$$

where R , F , L , and D_e are the gas constant, Faraday constant, the distance between blocking electrode and reversible electrode, and electronic diffusion constant respectively. D_e is given by the following equation using the diffusion coefficients of electrons (D_n) and holes (D_p) and concentration of electrons (n) and holes (p).

$$D_e = \frac{D_n n + D_p p}{n + p}, \quad (2)$$

D_e is equal to D_n when $n \gg p$, and D_e is D_p when $p \gg n$. From the partial conductivities of electrons (σ_n) and holes (σ_p) measured by dc-polarization, σ_n is much larger than σ_p in low P_{O_2} regime for 2TD-YSZ, 5TD-YSZ, and 10TD-YSZ.⁴⁻⁵⁾ D_n values can be estimated from the relaxation curves of high E_{app} , which is corresponding to low P_{O_2} , and D_p values from the curves of low E_{app} (high P_{O_2}). The mobility of electronic defects can be calculated from the diffusion coefficient by the Nernst-Einstein relation,

$$D_j = \frac{k}{e} \mu_j T, \quad (j=n, p), \quad (3)$$

where μ_n and μ_p are the mobilities of electrons and holes, and k and e are Boltzman constant and electronic charge, respectively. The model described above is abbreviated as W-model, hereafter.

Maruyama proposed a new model (M-model for abbreviation) for the analysis of the relaxation curves obtained by the non-steady state gas permeation measurements for non-doped YSZ, taking into account of the annihilation reaction of oxygen vacancies by the change of the oxygen fugacity profile in the electrolyte. Using the assumption of the linear profile of P_{O_2} in YSZ, the following relation has been derived,⁹⁾ when $\sigma_{O_2} \gg \sigma_p \gg \sigma_n$,

$$[(P_{O_2}^{\text{open}})^{1/4} - (P_{O_2}^{\text{rev}})^{1/4}] \left(\frac{dP_{O_2}^{\text{open}}}{dt} \right)^{-1} = \frac{FL^2}{8\mu_p RT} (P_{O_2}^{\text{open}})^{-3/4} + \frac{4FLV}{\sigma_p^0 A R^2 T^2} \quad (4)$$

where V , A , and σ_p^0 are volume of interior cavity of the polarization cell, electrode area, and the partial conductivity of holes at unit P_{O_2} , respectively. $P_{O_2}^{\text{open}}$ can be calculated using E_{open} by the following Nernst equation.

$$E_{\text{open}} = -\frac{RT}{4F} \ln \frac{P_{O_2}^{\text{open}}}{P_{O_2}^{\text{rev}}} \quad (5)$$

From the plot of $[(P_{O_2}^{\text{open}})^{1/4} - (P_{O_2}^{\text{rev}})^{1/4}] (dP_{O_2}^{\text{open}}/dt)^{-1}$ vs $(P_{O_2}^{\text{open}})^{-3/4}$, one can obtain μ_p and σ_p^0 simultaneously from the slope and the intercept of the plot, if the plot exhibits linear relationship. Therefore, μ_p and p at unit P_{O_2} (p^0), which can be calculated from the μ_p and σ_p^0 values using the relation of $\sigma_p^0 = e\mu_p p^0$, can be estimated from a single experiment. M-model can be extended to the calculation of the mobility of electrons. However, since erroneous results were obtain possibly due to the presence of buffering gas species

in the cavity, the analysis was only made for hole. Because of other limitations that the accurate value of the cavity volume is necessary and that σ_n is comparable or much higher than σ_p under the present experimental conditions for 10TD-YSZ. M-model was only applied for the analysis of μ_p in 5TD-YSZ.

III. Results and Discussions

3.1. Relaxation curves

Relationship between E_{open} and time (t) after the polarization circuit was open at 1273 K with the initial applied voltage (E_{app}) of 1.1 V under $P_{O_2}^{\text{rev}} = 1.0$ for 5TD-YSZ is shown in Fig. 1 (a). In the analysis using W-model (Eqs (1-1) and (1-2)), D_n values were calculated from the results of relaxation measurements in the E_{app} between 0.7 and 1.0 V for 10TD-YSZ, between 0.7 and 1.2 V for 5TD-YSZ, and between 1.3 and 1.6 V for 2TD-YSZ, respectively. D_n values were calculated from the plot of $E_{\text{open}} - t^{1/2}$ (Fig. 1 (b)) as well as the $E_{\text{open}} - t$ plot (Fig. 1 (a)) for the examination of the condition, $t \gg L^2/D_e$, since the total period of the relaxation measurements was about 5 s. D_p values were calculated from the results of relaxation measurements at D_p of 0.25 and 0.3 V for 5TD-YSZ and 0.5, 0.6 and 0.7 V for 2TD-YSZ. D_p values for 10TD-YSZ can not be calculated from the present results, since there is no E_{app} condition where σ_p is much larger than σ_n .⁴⁾ Fig. 2 (a) and Fig. 2 (b) shows $E_{\text{open}} - t$ and $E_{\text{open}} - t^{1/2}$ plots of the relaxation experiment at 1273K for 5TD-YSZ under the condition of $E_{\text{app}} = 0.25$ V and $P_{O_2}^{\text{rev}} = 1.0$.

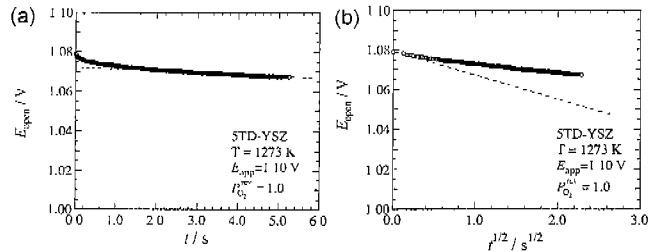


Fig. 1. Relationship between open circuit voltage, E_{open} and (a) time, t and (b) square root of time, $t^{1/2}$ by the non-steady state gas permeation measurements after the steady state at 1273 K under $E_{\text{app}} = 1.1$ V and $P_{O_2}^{\text{rev}} = 1.0$ for 5TD-YSZ.

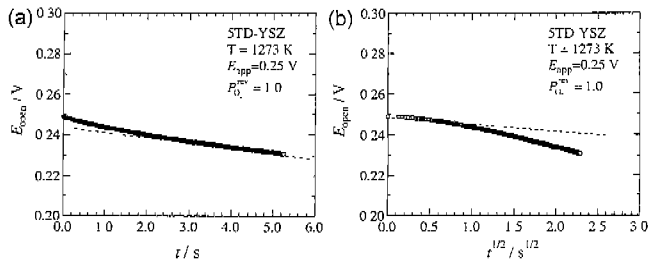


Fig. 2. Relationship between E_{open} and (a) t and (b) $t^{1/2}$ by the non-steady state gas permeation measurements after the steady state at 1273 K under $E_{\text{app}} = 0.25$ V and $P_{O_2}^{\text{rev}} = 1.0$ for 5TD-YSZ.

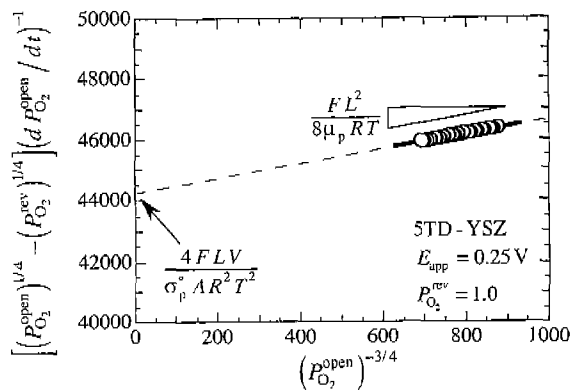


Fig. 3. Variation of $[(P_{O_2}^{open})^{1/4} - (P_{O_2}^{rev})^{1/4}](dP_{O_2}^{open}/dt)^{-1}$ with $(P_{O_2}^{open})^{-3/4}$ using the data obtained by the non-steady state gas permeation measurements after the steady state at 1273 K under $E_{app}=0.25$ V and $P_{O_2}^{rev}=1.0$ for 5TD-YSZ.

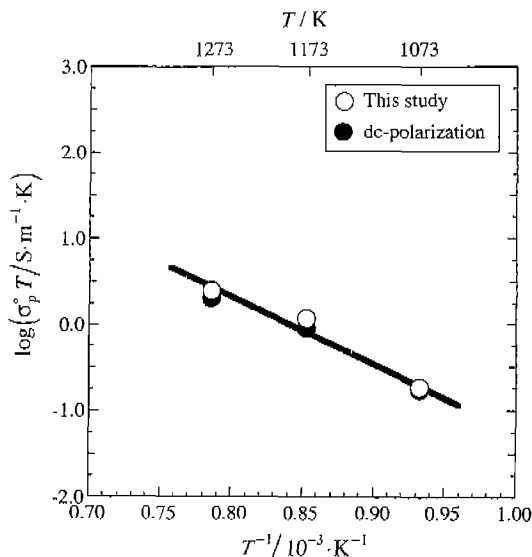


Fig. 4. Relationship between the product of the partial conductivity for holes at unit P_{O_2} (σ_p^0) and temperature, $\sigma_p^0 T$ and reciprocal temperature for 5TD-YSZ calculated by Eq. (4) shown by open circle. Reported $\sigma_p^0 T$ values estimated by the dc-polarization measurements³⁾ (closed circle) are also plotted for comparison.

In both cases for the estimation of electrons and holes, data of $t > 3$ s was used for the fitting using Eq. (1-1) and those of $t < 0.25$ s for Eq. (1-2).

On the other hand, the measurement period of 2TD-YSZ was longer than 100 s, which was long enough to assumed the condition of $t \ll L^2/D_e$. Therefore, the D_p and D_n values were calculated from the slope of E_{open} - t plot at $t > 30$ s in the case of 2TD-YSZ.

In the analysis using M-model (Eq. (4)), since linear relationships between $P_{O_2}^{open}$ and t is obtained from the experimental results, the value of $dP_{O_2}^{open}/dt$ was constant in each measurement.

As shown in Fig. 3, the plot of $[(P_{O_2}^{open})^{1/4} - (P_{O_2}^{rev})^{1/4}]$

$(dP_{O_2}^{open}/dt)^{-1}$ against $(P_{O_2}^{rev})^{-3/4}$ using the data in Fig. 2 (a) exhibits a good linear relationship. Arrhenius plot of $\sigma_p^0 T$ calculated from the intercept of the plot is shown in Fig. 4 for the comparison with $\sigma_p^0 T$ obtained separately by the dc-polarization measurements,³⁾ indicating the consistency of the M-model.

3.2 Mobility and concentration of holes

Arrhenius plots of $\mu_p T$ calculated by both W-model (Eqs. (1-1) and (1-2)) and M-model (Eq. (4)) for 2TD-YSZ, 5TD-YSZ, and 10TD-YSZ are summarized in Fig. 5. $\mu_p T$ for non-doped YSZ and CSZ are also plotted for comparison.⁸⁻¹¹⁾ $\mu_p T$ values for 5TD-YSZ by W-model show good agreement except for the result at 1073 K. $\mu_p T$ s calculated by M-model are larger by 0.5-1 order than those by W-model. Furthermore, the $\mu_p T$ values of 2TD-YSZ and 5TD-YSZ can be regarded to be identical, if one takes into account of the experimental errors. Reported μ_p values for non-doped YSZ by Maruyama⁹⁾ showed large difference with the present one.

Values of the activation energy for $\mu_p T(E_{\mu_p})$ of 5TD-YSZ are 1.39 eV by W-model and 1.23 eV by M-model. Those E_{μ_p} values seem to be too large for E_{μ_p} anticipated for the hopping conduction of small polarons, whose typical values range from 0.1 to 0.3 eV.¹²⁾ One possible explanation for such a high E_{μ_p} is the existence of hole traps as proposed by Maier.¹³⁾ However, further experiments will be necessary for detail discussion.

Arrhenius plot of p^0 calculated from μ_p and σ_p^0 for 2TD-YSZ and 5TD-YSZ is shown in Fig. 6. The p^0 values of non-doped YSZ and CSZ are also plotted for comparison.⁸⁻¹¹⁾ The p^0 values of 2TD-YSZ and 5TD-YSZ are smaller by about one order than the values of non-doped YSZ and CSZ. Values of the apparent activation energy for $p^0(E_p)$ in 2TD-YSZ and 5TD-YSZ are about 0.83 eV estimated by the W-model and 0.61 eV by M-model, and are almost independent of both TiO_2 concentration and model employed.

Although there are some differences in transport properties, such as the magnitudes of μ_p and p^0 values, between non-doped YSZ and TiO_2 -doped YSZ, the transport properties of holes in TiO_2 -doped YSZ are considered to be almost independent of TiO_2 concentration, since values of the σ_p^0 and the activation energy are almost independent of TiO_2 concentration.^{3-5, 8-10)}

3.3 Mobility and concentration of electrons

Fig. 7 shows the Arrhenius plot of $\mu_n T$ for 2TD-YSZ, 5TD-YSZ, and 10TD-YSZ calculated by W-model. $\mu_n T$ values of non-doped YSZ are also plotted in Fig. 7 for comparison.^{8,10,14,15)} Although the $\mu_n T$ values for 5TD-YSZ and 10TD-YSZ are found to be almost the same, $\mu_n T$ values for 2TD-YSZ are about a half order smaller than the values for 5TD-YSZ and 10TD-YSZ. The present results suggest that the electronic structure of conduction band in TiO_2 -doped YSZ is different from non-doped YSZ, which is supported by both electronic conductivity and optical measurements.³⁻⁵⁾

Activation energy of $\mu_n T$ for 2TD-YSZ, 5TD-YSZ, and

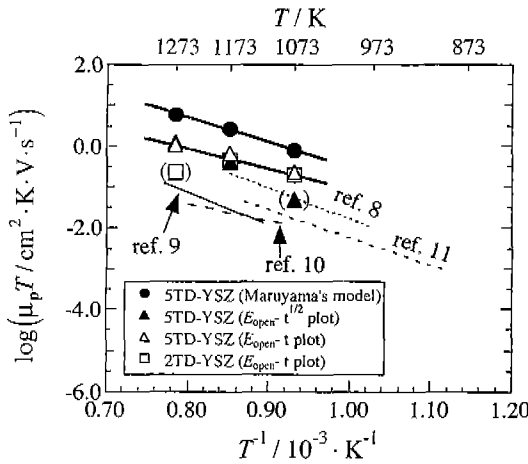


Fig. 5. Variation of product for the mobility of holes and temperature ($\mu_p T$) with reciprocal temperature for 2TD-YSZ and 5TD-YSZ. The $\mu_p T$ values of non-doped YSZ⁸⁻¹⁰ and CSZ¹¹ are also plotted for comparison.

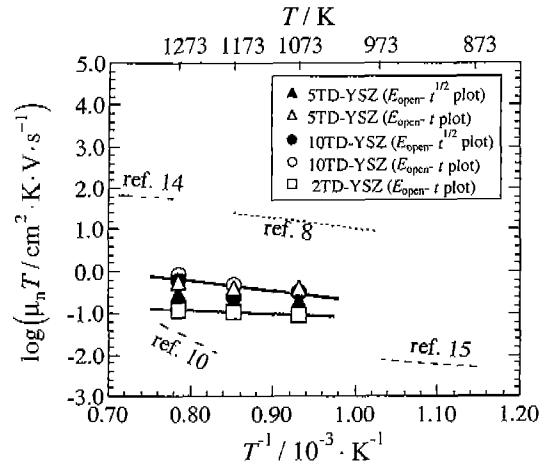


Fig. 7. Variation of product for the mobility of electrons and temperature ($\mu_n T$) with reciprocal temperature for 2TD-YSZ and 5TD-YSZ. The $\mu_n T$ values of non-doped YSZ^{8,10,14,15} are also plotted for comparison.

10TD-YSZ calculated from the slope of the Arrhenius plot, are 0.16, 0.19, and 0.38 eV, respectively, which are close to the value for a typical small polaron condition (0.3 eV).¹²

The concentration of electrons at unit $P_{O_2}(n^o)$ in 2TD-YSZ, 5TD-YSZ, and 10TD-YSZ are plotted in Fig. 8 in comparison with n^o values of non-doped YSZ.^{8, 10, 14, 15} n^o shows a strong dependency of TiO₂ concentration.

Oxygen nonstoichiometry (δ) and the concentration of the trivalent titanium ions ($[Ti_{Zr}']$) in $Zr_{0.852(1-x)}Y_{0.148(1-x)}Ti_xO_{1.926+0.07x-\delta}$ at 1273 K under $P_{O_2}=10^{-18}$ have been examined by both weight loss measurement and XPS analysis on the quenched sample. The values of δ and $[Ti_{Zr}']$ in $Zr_{0.772}Y_{0.134}Ti_{0.0094}O_{1.933-\delta}$, which of titanium composition is the same with 10TD-YSZ, are found to be 0.0129 and 0.0094, respectively. From the defect chemical consideration for TD-YSZ report-

ed in previous paper [3, 4], value of the concentration of electrons in TD-YSZ is determined by the following quasi-chemical reaction,



where $O_O^x, V_O^{\cdot\cdot}, e'$ are oxide ions on normal site, doubly-positive charged oxide vacancy, and free electron, respectively, and Ti_{Zr}^x and Ti_{Zr}' are neutral titanium ion, and single negatively-charged titanium ion on zirconium site, respectively. The concentration of free electron at 1273 K under $P_{O_2} = 10^{-18}$ (n^*) can be calculated from the following relationship using the volume of the unit cell (V) and Avogadro number (N),

$$n^* = \frac{2\delta - [Ti_{Zr}']}{V \cdot N} \tag{6}$$

n^* value in 10TD-YSZ can also be calculated by the following relationship, since n is proportional to $P_{O_2}^{-1/4}$,⁴

$$n^* = n^o \times 10^{-18} \tag{7}$$

The value of $\log(n^*/\text{mol}\cdot\text{m}^{-3})$ calculated by Eqs. (6) and (7) are 2.31 and 2.50 ± 0.03 , respectively, and both show a good agreement with each other.

The activation energy of $n^o(E_n)$ for 2TD-YSZ, 5TD-YSZ, and 10TD-YSZ calculated from the slope of the Arrhenius plot decreased with increasing TiO₂ concentration from 3.2, 2.5, to 2.6 eV, respectively. E_n values of 5TD-YSZ and 10TD-YSZ are found to be close to the value of TiO₂ (2.2 eV),¹⁶ while the E_n value of 2TD-YSZ is in the range between E_n values of non-doped YSZ and 5TD-YSZ or 10TD-YSZ. From the defect chemical view point, the E_n is given by the following relationship,¹⁷

$$E_n = \frac{1}{2}\Delta H_v \tag{8}$$

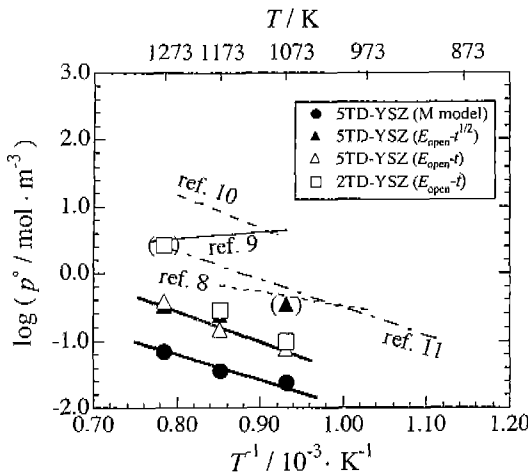


Fig. 6. Arrhenius plots of concentration for holes at unit $P_{O_2}(p^o)$ calculated from μ_p shown in Fig. 5 and the partial conductivity for holes at unit P_{O_2} , measured by the dc-polarization measurements. The p^o values of non-doped YSZ⁸⁻¹⁰ and CSZ¹¹ are also plotted for comparison.

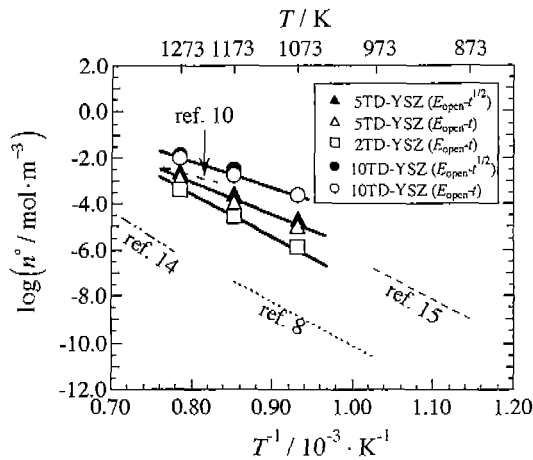


Fig. 8. Arrhenius plots of concentration for electrons at unit $P_{O_2}(n^0)$ calculated from μ_n shown in Fig. 7 and the partial conductivity for electrons at unit P_{O_2} measured by the dc-polarization measurements. The n^0 values of non-doped YSZ^{8,10,14,15} are also plotted for comparison.

where ΔH_v is the enthalpy change for the quasi-chemical reaction (A). The experimental fact that the ΔH_v values of 5TD-YSZ and 10TD-YSZ are closed to that of TiO_2 suggests that the oxide ion vacancy is preferably formed in the neighbouring sites of Ti ions. Similar suggestion is reported for YSZ doped with Nb_2O_5 or MnO_2 doped YSZ.⁶ The decrease in ΔH_v leads to the increase of the concentration of V_O and n from Eq. (A), since the increase of n by the TiO_2 doping is estimated as being responsible for the increase in the partial conductivity of electrons.

IV. Conclusions

Mobilities of electrons and holes in 2TD-YSZ, 5TD-YSZ, and 10TD-YSZ were estimated from the non-steady state gas permeation measurements employing the models proposed by Weppner and Maruyama. Also the concentrations of electrons and holes at unit P_{O_2} have been calculated from the mobility and the partial conductivities at unit P_{O_2} . The mobilities and the activation energies of electrons and holes are almost independent of TiO_2 concentration. In contrast, n^0 and μ_n show a strong TiO_2 -concentration dependence that n^0 increase with increasing TiO_2 concentration. μ_n values of 5TD-YSZ and 10TD-YSZ are slightly larger than those of 2TD-YSZ. The E_n value decreases by the addition of TiO_2 , approaching to the value of TiO_2 .

References

1. S. S. Liou and W. L. Worrell, "Electrical Properties of Novel Mixed-conducting Ceramics," *Appl. Phys. A*, **49**, 25-31 (1989).
2. A. Kopp, H. Nafe, W. Weppner, P. Kountouros and H. Schubert, "Ionic and Electronic Conductivity of TiO_2 - Y_2O_3 -

3. Stabilized Tetragonal Zirconia Polycrystals," in Proceeding of the International Conference on Zirconia V, Ed. S. P. S. Badwal, M. J. Bannister and R. H. J. Hannink (Technomic, Landaster, PA, 1993), pp. 567-575.
4. K. Kobayashi, Y. Kai, S. Yamaguchi, N. Fukatsu, T. Kawashima and Y. Iguchi, "Electronic Conductivity Measurements of 5 mol% TiO_2 Doped YSZ by a Dc-polarization Technique," *Solid State Ionics*, **93**, 193-199 (1997).
5. K. Kobayashi, Y. Kai, S. Yamaguchi, N. Fukatsu, T. Kawashima and Y. Iguchi, "Partial Conductivity of YSZ Doped with 10 mol% TiO_2 ," *J. Kr. Ceram. Soc.*, **4**, 114-121 (1998).
6. K. Kobayashi, S. Yamaguchi, T. Higuchi, S. Shin and Y. Iguchi, "Electronic Transport Properties and Electronic Structure of TiO_2 -Doped YSZ," Accepted in *Solid State Ionics*.
7. X. J. Huang and W. Weppner, *J. Chem. Soc.*, "Characteristics of Transition Metal Oxide Doping of YSZ: Structure and Electrical Properties," *Faraday Trans.*, **92**, 2173-2178 (1996).
8. W. Weppner, "Electronic Transport Properties and Electrically Induced p - n Junction in ZrO_2 +10 m/o Y_2O_3 ," *J. Solid State Chem.*, **20**, 305-314 (1977).
9. W. Weppner, "Electrochemical Transient Investigations of the Diffusion and Concentration of Electrons in Yttria Stabilized Zirconia-solid Electrolytes," *Z. Naturforsch.*, **31a**, 1336-1343 (1976).
10. T. Maruyama, "Electron-hole Concentration in Yttria-stabilized Zirconia," Abstract of the 60th meeting of Japanese electrochemical society, Tokyo, p. 106, 1993.
11. J. H. Park and R. N. Blumenthal, "Electronic Transport in 8 Mol Percent Y_2O_3 - ZrO_2 ," *J. Electrochem. Soc.*, **136**, 2867-2876 (1989).
12. L. Heyne and N. M. Beekmans, "Electronic Transport in Calcia-stabilized Zirconia," *Proc. Brit. Ceram. Soc.*, **19**, 229-263 (1970).
13. I. G. Austin and N. F. Mott, "Polarons in Crystalline and Non-crystalline Materials," *Adv. Phys.*, **18**, 41-102 (1969).
14. J. Maier, "Mass Transport in the Presence of Internal Defect Reactions-concept of Conservative Ensembles: III, Trapping Effect of Dopants on Chemical Diffusion," *J. Am. Ceram. Soc.*, **76**, 1223-1227 (1996).
15. L. D. Burke, H. Rickert and R. Steiner, "Elektrochemische Untersuchungen zur Teilleitfähigkeit, Beweglichkeit und Konzentration der Elektronen und Defektelektronen in dotiertem Zirkondioxid und Thoriumdioxid," *Z. Phys. Chem (NF)*, **74**, 146-167 (1971).
16. A. Kopp, H. Nafe and W. Weppner, "Characterization of the Electronic Charge Carrier in TZP," *Solid State Ionics*, **53-56**, 853-858 (1992).
17. J.-F. Marucco, J. Barutron and P. Lemasson, "Thermogravimetric and Electrical Study of Non-stoichiometric Titanium Dioxide TiO_{2-x} between 800 and 1100°C," *J. Chem. Phys. Solids*, **42**, 363-367 (1981).
18. S. Yamaguchi, K. Kobayashi, Y. Iguchi, N. Yamada and T. Kato, "Electronic Transport Properties of $ZrTiO_4$ at High Temperature," *Jpn. J. Appl. Phys.*, **33**, 5471-5476 (1994).